TASK QUARTERLY 5 No 2 (2001), 125–140

THERMO-MECHANICAL COUPLING BETWEEN THE FLOW OF STEAM AND DEFORMATION OF THE VALVE DURING START-UP OF THE 200 MW TURBINE

MARCIN BIELECKI[1], MICHAŁ KARCZ[1], WOJCIECH RADULSKI[2] AND JANUSZ BADUR[1]

[1] *Institute of Fluid-Flow Machinery, Polish Academy of Sciences, Reacting Flow Department, Fiszera 14, 80-952 Gdansk, Poland*
jb@imp.gda.pl

[2] *Alstom Power, Stoczniowa 2, 82-300 Elbląg, Poland*

(Received 20 August 2000; revised manuscript received 10 January 2001)

Abstract: The lifetime estimation of power station structures and components, subjected to fatigue loading, is essential for determining the moment of repair or replacement. Therefore the degradation behaviour and damage development within material should be very well understood. This research focuses on a fluid-solid interaction that has been developed in Finite Volume Method software for description of heat and flow loading on a cut-off valve and Finite Element Method software for conduct researches on fatigue and creep damage of the valve material.

Keywords: fluid-solid interactions, compressible flow, heat, creep, damage, fatique, FEM, FVM, stresses

1. Introduction

Elements of constructions in modern power plants, especially in supercritical steam power plants, cogeneration installation, combined cycle power plants are frequently subjected to severe unsteady thermal and mechanical stresses. Repeated loading due to start-up and shutdown or normal one-day operation cycle usually lead to degradation of material owing to intensive interactions of many failure modes such as local plasticity, high tepertature creep, damage, corrosion, fatigue and cracking. Interactions of main modes of degradation are complex in appropriate numerical modelling and difficult for the numerically based life time predictions. For instance, creep and damage can be intensified by the process of locally variable high thermal stresses during cycles of loading and unloading.

Growing demands on safe, reliable and economic operation ask for a sufficient lifetime prolongation of the critical power plant elements, therefore it is necessary to develop numerical studies related to better description of the thermo-mechanical coupling [1, 2]. In

order to account for the complex flow in the elements under consideration a compressible, viscous, conductive, turbulent, 3D Finite Volume Element code with a thermal boundary layer modelling, based on classical wall functions should by applied. In this case, the main aim of Computational Fluid Dynamics (CFD) is to accurately compute both the steam temperature and the steam-metal heat transfer coefficients during every stage of start-up and shutdown. A key point of CFD analysis is to predict a correct rate of heating important for determination of transient thermal stresses at the unsteady operation. So as to account for complex unsteady deformation of creeping, damaging, and stress corrosion cracking of material a full analysis of thermal stresses state should be performed using a 3D code of Computational Structural Mechanics or Computational Solid Mechanics (CSM).

The present paper undertakes the effort of application of an integrated CFD-CSM analysis for prediction of the rate of degradation of a cut-off valve in a 200 MW Steam Power Plant. The valve under consideration has been experimentally tested at laboratory [3] and at the Power Plant Kozienice [4].

1.1. Specifics of CFD – CSM interactions

Due to the combination of physical complexity with 3D geometry of structural elements, analytical solutions becomes inappropriate for analysis, and therefore numerical methods have to be applied. As, both, the Finite Element and Finite Volume Methods are now commonly used, the computer code ABAQUS^{TM}, which is of high flexibility allowing for users' modelling of materials, together with FLUENT^{TM}, which is a powerful tool in fluid and heat flow analysis, are employed. Performed here, a numerical example of the cut-off valve illustrates the main features of CFD – CSM interaction in the circumstances under consideration. In Figure 1 the main points of a coupled description based on using similar discretization meshes for both CFD and CSM are schematically presented.

This approach has some advantages, including facility of numerical application, and appears to describe creep, thermo-mechanical behaviour, stress-strain relationship and lifetime quite well. This includes damage under uniaxial loading as seen on carried out numerical tests [4–7].

1.2. Governing equations in the conservative form

The fundamental equation of CFD and CSM can be written in the following eulerian, basic form:

$$\frac{\partial}{\partial t}\mathbf{U} + \nabla \cdot \mathbf{F}^{\mathbf{c}} = \nabla \cdot \mathbf{F}^{\mathbf{v}} + \mathbf{S} \tag{1}$$

where:

U – vector of conservative variables,

$\mathbf{F}^{\mathbf{c}}$ – convective fluxes,

$\mathbf{F}^{\mathbf{v}}$ – diffusive fluxes,

S – sources vector.

The conservative variables vector, usually is defined as [8, 9]:

$$\mathbf{U} = \begin{Bmatrix} \rho \\ \rho \vec{v} \\ \rho e \\ \rho Y_K \end{Bmatrix} \begin{matrix} mass \\ momentum \\ energy \\ evolution\ of\ microstructure \end{matrix} \tag{2}$$

The parameter Y_K (scalar, vector or tensor) indicates an evolution of different microstructures ($K = 1, \ldots, N$). For CFD balance equations those parameters can describe evolution of

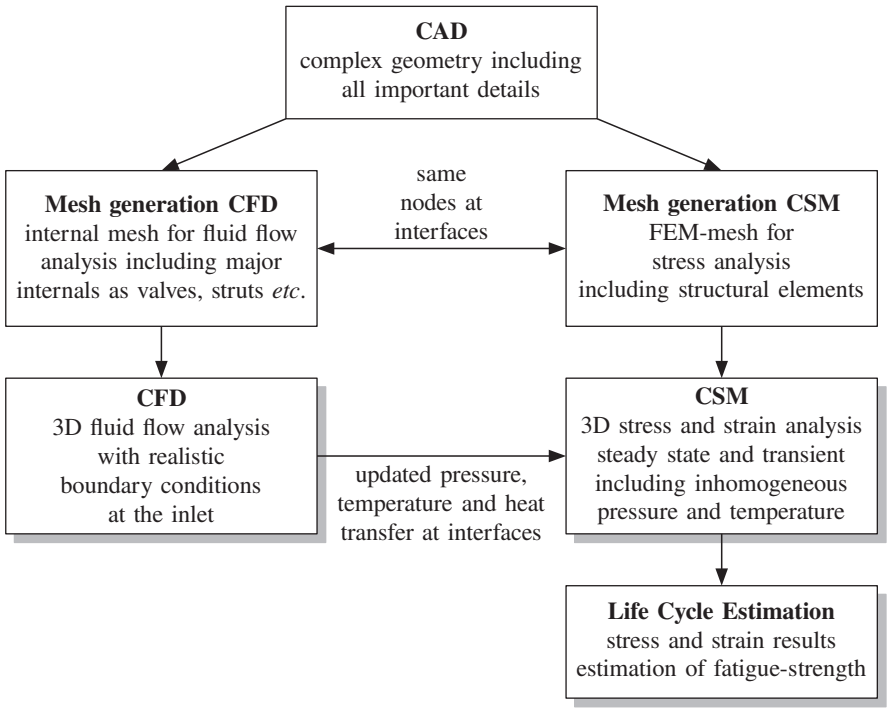

Figure 1. Scheme of solid-fluid coupling in the analysis

the turbulent kinetic energy k, the turbulent dissipation rate ε or the mixture component, the mass fraction, *etc*. In the case of CSM, parameters Y_K can express evolution of the creep inelastic deformation $\overleftrightarrow{\varepsilon_{cr}}$, the damage ω, the shift tensor $\overleftrightarrow{\alpha}$, *etc*.

The evolution equations of these mentioned parameters can be written in the following form that is common for both cases – CFD and CSM:

$$\frac{\partial}{\partial t}(\rho Y_K) + \nabla \cdot \left(\rho \overrightarrow{\upsilon} Y_K\right) = \nabla \cdot \overrightarrow{J_K} + \rho S_K \tag{3}$$

where ρ is density, $\overrightarrow{v}$ – velocity, $\overrightarrow{J_K}$, S_K – the flux and the sources of microstructure, respectively.

1.2.1. FVM – Finite Volume Method – the governing equations

The form of the governing equations in Finite Volume Method (FLUENT) is the same for both fluid and solid part of a computational domain. The different number of flow modes can be predicted using this method *i.e.* steady or unsteady, compressible or incompressible, inviscid or viscous with different turbulence model, *etc*. It is also possible to compute heat transfer between fluid and solid region or heat conduction in solid material, which is represented by equation of balance of energy (10).

The set of governing equations can be expressed in different forms for fluid and solid regions as follows:

(a) FLUID

$$\frac{\partial}{\partial t}\begin{Bmatrix}\rho\\ \rho\overrightarrow{\upsilon}\\ \rho e\\ \rho k\\ \rho\varepsilon\end{Bmatrix}+\nabla\cdot\begin{Bmatrix}\rho\overrightarrow{\upsilon}\\ \left(\rho\overrightarrow{\upsilon}\otimes\overrightarrow{\upsilon}\right)+p\overleftrightarrow{I}\\ (\rho e+p)\overrightarrow{\upsilon}\\ \rho\overrightarrow{\upsilon}k\\ \rho\overrightarrow{\upsilon}\varepsilon\end{Bmatrix}=\nabla\cdot\begin{Bmatrix}0\\ \overleftrightarrow{\tau}^{c}\\ \overleftrightarrow{\tau}^{c}\overrightarrow{\upsilon}+\overrightarrow{q}^{c}\\ \overrightarrow{J_k}\\ \overrightarrow{J_\varepsilon}\end{Bmatrix}+\begin{Bmatrix}0\\ \rho\overrightarrow{b}\\ \rho S_e\\ \rho S_k\\ \rho S_e\end{Bmatrix} \tag{4}$$

where:

ρ – density of fluid,
$\overrightarrow{\upsilon}=\upsilon_x\overrightarrow{e_x}+\upsilon_y\overrightarrow{e_y}+\upsilon_z\overrightarrow{e_z}$ – velocity of fluid,
p – termodynamical pressure,
$\rho\overrightarrow{v}\otimes\overrightarrow{v}$ – convective momentum flux,
$\overleftrightarrow{I}=\delta_{ij}\overrightarrow{e_i}\otimes\overrightarrow{e_j}=$ $=\overrightarrow{e_x}\otimes\overrightarrow{e_z}+\overrightarrow{e_y}\otimes\overrightarrow{e_z}+\overrightarrow{e_x}\otimes\overrightarrow{e_y}$ – Gibbs' idemfactor $\{i,j=x,y,z\}$,
$e=c_pT_i+\frac{1}{2}\overrightarrow{v}\cdot\overrightarrow{v}$ – total energy,
$\overleftrightarrow{\tau}^{c}$ – total, irreversible momentum flux,
$\overrightarrow{q}^{c}$ – total heat flux,
$\overrightarrow{b}$ – mass force,
k – turbulent kinetic energy,
ε – dissipation rate of turbulent kinetic energy,
$\overrightarrow{J_k}$ – diffusive flux of k,
$\overrightarrow{J_\varepsilon}$ – diffusive flux of ε,
ρS_k, ρS_ε, ρS_e – sources of k, ε and energy respectively,
$\nabla=\overrightarrow{e_x}\frac{\partial}{\partial x}+\overrightarrow{e_y}\frac{\partial}{\partial y}+\overrightarrow{e_z}\frac{\partial}{\partial z}$ – Hamilton's operator.

The total irreversible momentum flux can be divided into different dissipative parts (viscous, turbulent, diffusive, radiation, transpiration):

$$\overleftrightarrow{\tau}^{c}=\overleftrightarrow{\tau}+\overleftrightarrow{r}+\overleftrightarrow{\tau}^{dyf}+\overleftrightarrow{\tau}^{rad}+\overleftrightarrow{\tau}^{trans} \tag{5}$$

The first of them is known as a tensor of molecular viscosity stresses which is defined as:

$$\overleftrightarrow{\tau}=\left[\mu\left(\frac{\partial\upsilon_i}{\partial x_j}+\frac{\partial\upsilon_j}{\partial x_i}\right)-\frac{2}{3}\mu\frac{\partial\upsilon_k}{\partial x_k}\delta_{ij}\right]\overrightarrow{e_i}\otimes\overrightarrow{e_j} \tag{6}$$

Turbulent flux of momentum, known as the Reynolds stress tensor, can be simply defined in analogy to Equation (6):

$$\overleftrightarrow{r}=\left[-\overline{\rho'\upsilon_i'\upsilon_j'}\right]\overrightarrow{e_i}\otimes\overrightarrow{e_j}=\left[\mu_T\left(\frac{\partial\upsilon_i}{\partial x_j}+\frac{\partial\upsilon_j}{\partial x_i}\right)-\frac{2}{3}\left(\rho k+\mu_T\frac{\partial\upsilon_k}{\partial x_k}\right)\delta_{ij}\right]\overrightarrow{e_i}\otimes\overrightarrow{e_j} \tag{7}$$

The total heat flux can also be divided into different parts similarly as it in the case of the flux of momentum. The turbulent part of total heat flux can be written in analogy with the Reynolds stress tensor in the form based on Fourier's Law:

$$\overrightarrow{q}^{turb}=\overline{\rho'\upsilon_i'T'}=\lambda_T\nabla T \tag{8}$$

where $\lambda_T=f(\mu_T)$ is a turbulent heat transfer coefficient. Parameter μ_T is a turbulent viscosity coefficient and it can be defined as:

$$\mu_T=C_\mu\rho\frac{k^2}{\varepsilon} \tag{9}$$

(b) SOLID

$$\frac{\partial}{\partial t}\begin{Bmatrix}0\\0\\\rho h\\0\\0\end{Bmatrix}+\nabla\cdot\begin{Bmatrix}0\\0\\0\\0\\0\end{Bmatrix}=\nabla\cdot\begin{Bmatrix}0\\0\\\lambda\nabla T\\0\\0\end{Bmatrix}+\begin{Bmatrix}0\\0\\q_{in}\\0\\0\end{Bmatrix} \tag{10}$$

where [9]:

ρ – density of solid material,
λ – thermal conductivity,
q_{in} – heat sources,
$h=\int_{T_{ref}}^{T} c_p dT$ – sensible enthalpy.

1.2.2. FEM – Finite Element Method – the governing equations

The set of governing equations for Finite Element Method (ABAQUS) is very similar in its form to the Finite Volume Method that is described above.

$$\frac{\partial}{\partial t}\begin{Bmatrix}0\\\rho\vec{\upsilon}\\\rho e\\\rho\overleftrightarrow{\varepsilon}_{cr}\\\rho\omega\end{Bmatrix}+\nabla\cdot\begin{Bmatrix}0\\\left(\rho\vec{\upsilon}\otimes\vec{\upsilon}\right)+\overleftrightarrow{\sigma}\\\rho e\vec{\upsilon}\\\rho\overleftrightarrow{\varepsilon}_{cr}\vec{\upsilon}\\\rho\omega\vec{\upsilon}\end{Bmatrix}=\nabla\cdot\begin{Bmatrix}0\\0\\\overleftrightarrow{\sigma}\vec{\upsilon}+\vec{q}\\0\\\vec{J}_{\omega}\end{Bmatrix}+\begin{Bmatrix}0\\\rho\vec{b}\\\rho S_e\\\rho S_{cr}\\\rho S_{\omega}\end{Bmatrix} \tag{11}$$

where:

ρ – density of solid,
$\vec{\upsilon}=\upsilon_x\vec{e_x}+\upsilon_y\vec{e_y}+\upsilon_z\vec{e_z}$ – velocity of solid,
$\overleftrightarrow{\sigma}$ – recoverable stresses,
$\overleftrightarrow{\varepsilon}_{cr}$ – creep inelastic deformation,
ω – damage parameter.

Creep is a property of steel that is important in high-temperature, under cyclic service. Above approximetly 500°C there is a drop in the strength of steel and with a constant load at the elevated temperature, permanent deformation takes place owing to the inelastic nature of the material. Long-time exposure to conditions of creep will cause unacceptable deformations, and even rupture or tearing of the material. It is necessary to establish permissible times of creep and creep rates to avoid such situations. The rate of the creep strain tensor is formulated as an anisotropic incompressible inelastic flow [10] expressed in the function of the stress deviator s_{ij} and the shift tensor α_{ij}:

$$\frac{\partial}{\partial t}\varepsilon_{ij}^{cr}+\frac{\partial}{\partial x_k}\left(\varepsilon_{ij}^{cr}\upsilon_k\right)=\frac{3}{2}\frac{\dot{\varepsilon}^{cr}}{\sigma_M}\left(s_{ij}-\alpha_{ij}\right) \tag{12}$$

The rate of the uniaxial creep strain is given by the extended unsteady Norton rule [11]:

$$\frac{\partial}{\partial t}\varepsilon^{cr}+\frac{\partial}{\partial x_k}(\varepsilon^{cr}\upsilon_k)=A\left[\frac{\sigma_M(1+\lambda\varepsilon^{cr})}{(1-\omega)}\right]^{m(T)} \tag{13}$$

The kinematic deviatoric shift tensor α_{ij} that is the position of the centre of the creep yield surface in stress space depends on history of inelastic strain state [11]:

$$\dot{\alpha}_{ij}=H\dot{\varepsilon}_{ij}^{cr} \tag{14}$$

$$H = \begin{cases} C & \text{if } \sqrt{\frac{3}{2}\alpha_{ij}\alpha_{ij}} \le 0.3\sigma_y \\ 0 & \text{if } \sqrt{\frac{3}{2}\alpha_{ij}\alpha_{ij}} > 0.3\sigma_y \end{cases} \tag{15}$$

where:

σ_y – yield stress,
s_{ij} – the stress deviator,
σ_M – the Huber-Mises equivalent stress,
C – slope of uniaxial stress versus inelastic strain curve;

for linear inelastic strain hardening rule:

$$C = \frac{\sigma_u - \sigma_y}{\varepsilon_u - \frac{\sigma_u}{E}} \tag{16}$$

ε_u – elongation related to ultimate stress,
σ_u – ultimate stress *i.e.* strength in tension,

and material parameters are: C, A, $m(T)$ [11].

The damage evolution equation is as follows [12]:

$$\frac{\partial}{\partial t}\omega + \frac{\partial}{\partial x_k}\omega v_k = \frac{\partial}{\partial x_k}(\chi\omega_k) + \left[\frac{\sigma_M(1+\lambda\varepsilon^{cr})}{\sigma_u(1-\omega)}\right]^{n(T)} \tag{17}$$

where $\sigma_u(T)$ is the ultimate strength which depends on temperature, χ is damage propagation coefficient (here taken to be zero) and an arbitrary parameter $\lambda = \{-1, 1\}$.

2. Cold start-up of the cut-off value

The start-up of a turboset from its cold state always causes serious problems and seems to be a complex phenomenon that is connected with a rate and frequency of the start-up. A good knowledge of the material stress behaviour due to this is very important and its prediction can simply optimise the way of correct turboset cold start-up and allows to avoid different states of emergency for the whole power station.

The valves, shafts and turbine casings are the most stressed thick-wall parts of the turbosets. During cold start-up these elements are loaded unsteadily both mechanically (pressure, centrifugal forces due to the rotation of the shaft) and thermally (heat transfer between steam and imposed surface). Depending on the rate of the wall temperature growth there appear unsteady thermal stresses that can be amplified by mechanical ones.

The evolution of the main parameters as load rate, temperature and pressure of the live steam at the admission and rotational speed of the turbine shaft during start-up operation for 200 MW turboset are showed in simplified common diagram – Figure 2 [6].

The main task of the current work is to employ the two different numerical codes, which connected together can in a reliable way predict different thermal states of the particular turboset part as the main cut-off valve during start-up[1]. The valve of this type is the first element on steam flow-path from boiler to turbine[2] so it is clearly seen that this

1. One of the first works that coupled numerically aerodynamic and thermodynamic behaviour of turbine elements was conducted by DEJEAN and BRUCHET in 1995 [1, 2]. These papers dealed with calculation of bucket root and diaphragm packing leakage flow of HP second stage of the impulse 250 MW fossil fired steam turbine and its rotor creep – fatigue damage prediction during the cold start-up.

2. Excluding an admission pipe.

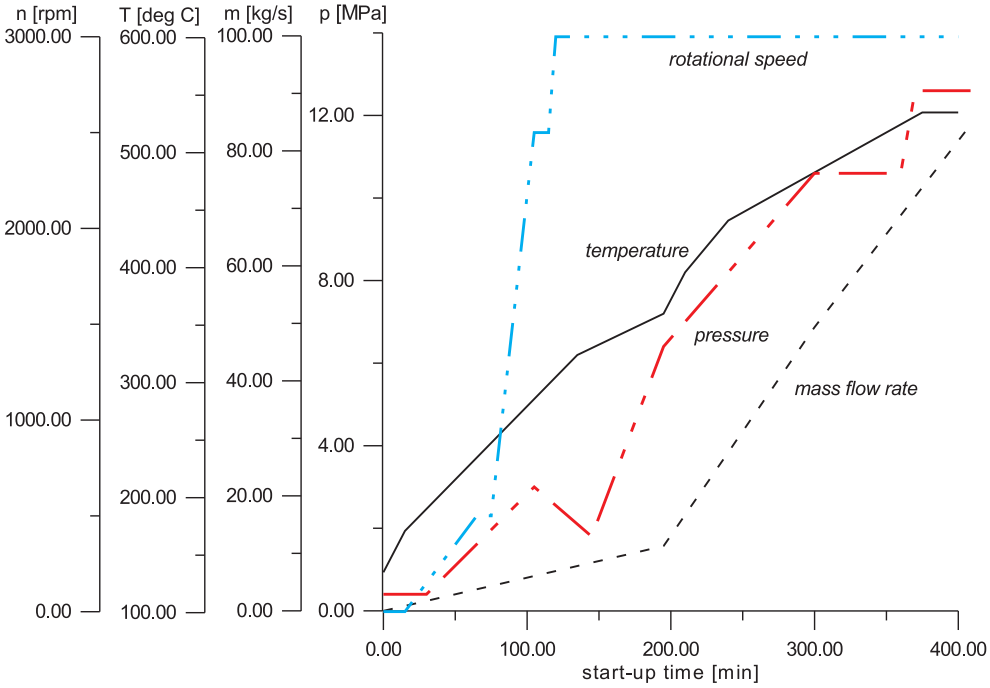

Figure 2. A simplified start-up diagram of 200 MW turbosets

facility is the most exposed to transient thermal stresses during start-up due to the highest temperature of steam. It is very important to avoid some work disturbances of this valve because it is one of the main emergency facilities in power station.

In Figure 3 the simplified geometry of a cut-off valve at the 200 MW unit of Power Plant Kozienice has been shown, which is, usually, a critical element in the start-up loading process.

3. Calculation of steam flow and heating during start-up

Calculations of flow through the cut-off valve have been carried out with commercial software package FLUENT [12] that has been used in Reacting Flow Department of IFFM PAS-ci since 1997.

Calculations of flow and heat transfer phenomenon were performed for the whole 3D geometry of cut-off valve – steam flow part and steel casing part simultaneously. It is possible by using one energy equation which ”spreads” on both inner ”fluid” and outer ”solid” parts of valve. This procedure allowed us to calculate heat transfer between steam and a casing of the valve. Investigation of a rapid growth and unequal distribution of valve temperature, pressure and velocity during start-up of a turboset has been a major task of current numerical calculations.

For numerical simulations 3D an unsteady flow model and segregated solver were assumed. An unstructured grid of 80 000 to 200 000 tetrahedral finite volumes refined generally between head and seat of the valve was employed for discretization of the flow domain. It was necessary to pay special attention to the proper refining of the mesh between head and seat and nearby the walls. There were used procedures which allowed for receiving

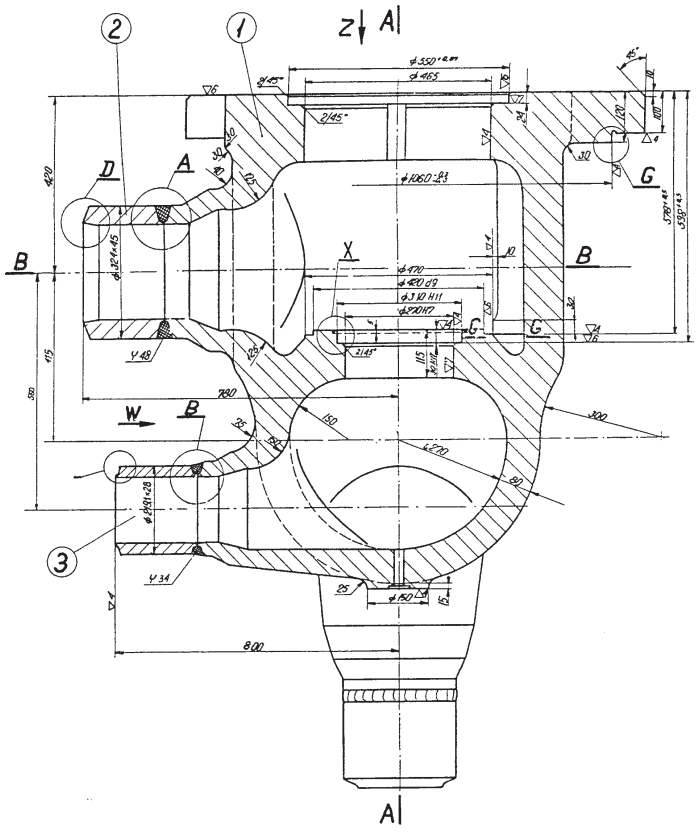

Figure 3. View on the geometry of the cut-off valve

a proper value of non-dimensional parameter y^+. In order to correctly model the logarithmic thermal sub-layer and the conductive thermal sublayer, the mesh is stretched close to the wall. For these refined grid $y^+ \equiv \rho u y/\mu$ is smaller than 60 and bigger than 30 [13]. The first grid node is located in the logarithmic sub-layer. A general overview of the surface outer – inner mesh is presented in Figure 4.

Flow has been modelled by the so-called Navier-Stokes equations for viscous conducting fluid (Equation 4). The flowing gas – water vapour – was treated as a compressible medium and its thermodynamic properties were calculated from the thermal and caloric equation for perfect gas which is adequate for a superheated steam ($R = 461.5$ J/kg·K, $\kappa = 1.3$), [5]. The constant values of specific heat, viscosity, thermal conductivity and Prandtl number (0.94) for steam at equilibrium conditions at the mean level of pressure and temperature (180 bar, 540°C) has been imposed.

The standard well known $k - \varepsilon$ turbulence model was chosen to simulate the gas turbulent fluctuations. This model is generally valid for industrial fully turbulent high-Reynolds-number flows [14, 1, 6]. The standard wall functions model was employed for near wall region treatment.

Thermal conductivity and specific heat coefficients of the L21HMF steel body valve were prepared in the form of polynomial equations in their dependence from local

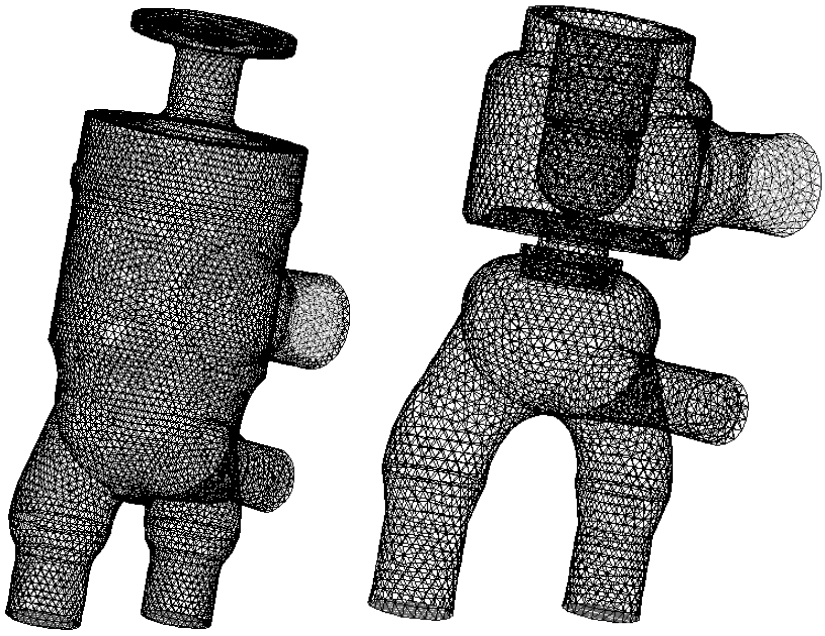

Figure 4. Overview of the calculation grid on the valve outer and inner surfaces

temperature. These equations and value of other material properties (density and modulus of elasticity) are as follows [12, 15]:

$$\begin{aligned} c(T) &= 460 + 0.177 \cdot T + 4.67 \cdot 10^{-4} \cdot T^2 && [\mathrm{J/kg \cdot K}] \\ \lambda(T) &= 44.2 - 0.0088 \cdot T - 2.21 \cdot 10^{-5} \cdot T^2 && [\mathrm{W/m \cdot K}] \\ \rho &= 7850 && [\mathrm{kg/m^3}] \\ E &= 2 \cdot 10^5 \left(0.987 + 0.301 \cdot 10^{-3} T - 1.857 \cdot 10^{-6} T^2\right) && [\mathrm{MPa}] \end{aligned} \tag{18}$$

Figure 5 shows the calculated steam velocity magnitude on the end of the start-up process (after 400 min.) distributed on the symmetry plane and two main cross sections. Figure 6 shows computed steam and casting temperature after 400 min. of start-up. We observe a near constant temperature along the mean stream (540–520°C) and decrease of wall temperature in places where pressure decreases. The values of heat transfer coefficient along the inter surfaces, generally, is increasing in the time of start-up, reaching after 400 min. values in different points 10 000–60 000 W/m^2°C.

The computed local coefficients of heat transfer are similar to those based on experimentally elaborated analytical laws [3, 15]. The locally observed discrepancies (smaller analytically predicted heat transfer) are due to the fact that the numerical solution takes into account more complex geometry of inner channels of the valve.

4. **Transient thermal stresses**

The structure has been analysed thermo-mechanically by Finite Elements Method software ABAQUS, and it has been considered as an axisymmetrical substructure, made of circa 4 000 (3 500 nodes) axisymmetric low order elements with full thermal-displacement coupling (Figure 7). The valve material is the ferritic stainless steel CrMoV (L21HMF) changing the Young's modulus from 210000 MPa at 20°C to 150000 MPa at 550°C (see Equation (18_4)) and the yield stress from 750 MPa at 20°C to 315 MPa at 550°C. Figure 8

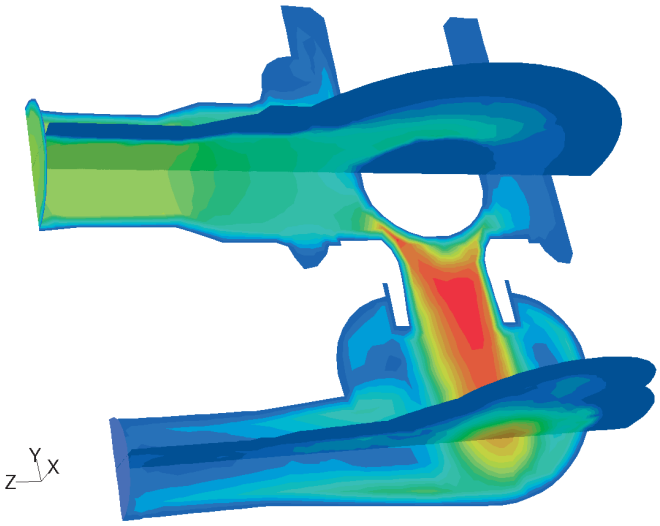

Figure 5. The distribution of the velocity magnitude in the symmetry plane and two planes perpendicular to each other

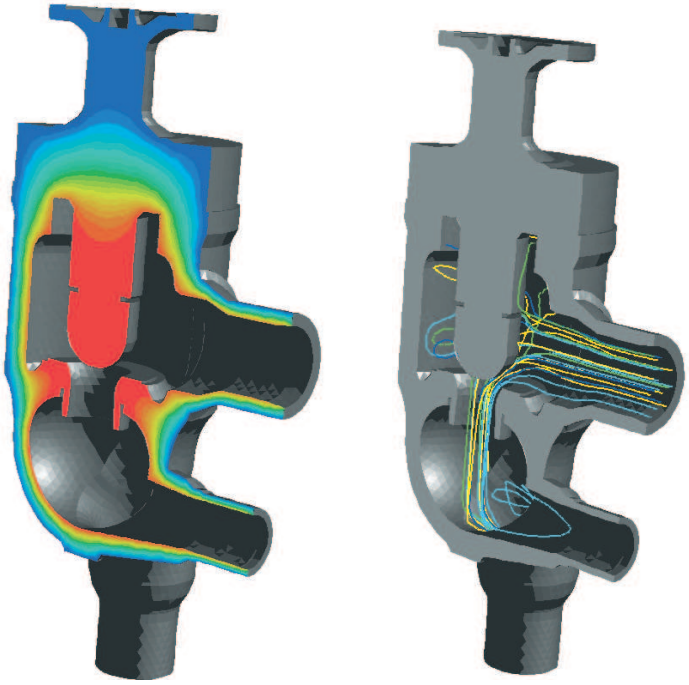

Figure 6. The distribution of the temperature in the symmetry plane of the cut-off valve and path line coloured by velocity magnitude

shows temperature profile in the valve casing which is radially stratified and, as we have observed, during the start-up it becomes progressively axially stratified. During start-up, by transient calculations, thermo-mechanical stresses as well as their time evolution were also performed [4]. Figure 9 shows the steady-state thermo-mechanical stresses which are

far from the yield stresses. However, at the start-up operation the comprehensive thermal stresses, due to the rate of gradient of temperature (Figure 10) exceeding the yield stress in the point F. It means, that after shutdown the small residual tensile stresses are present at this place, resulting from plastic compression.

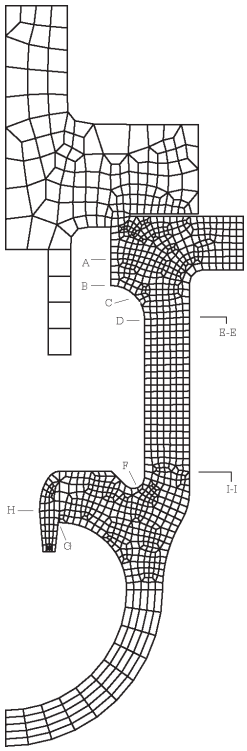

Figure 7. Finite elements mesh for solid analysis with ABAQUS software

It has been found that due to anisothermal warm-up whole peaks of enormous stresses have a maximum approximately after 60 min. after start up as shown in Figure 10. The difference in temperature between inner side wall which is warmed-up quickly and the outer side leads to maximal values of thermal effective stresses below 100 MPa.

5. **High temperature creep after start-up**

In creep conditions the service time plays an essential role in the evaluation of structures behaviour. Even under constant load much below plastic level microstructural changes occur in a material. This results in two basic phenomena: steadily growing deformations and gradual material deterioration. From an engineering point of view both may preclude structures' usefulness *i.e.* they may miss design criteria for a given exploitation time. The evaluation of a safe exploitation time becomes then the main task in designing structures, which are expected to undergo such conditions. Thus many researches are devoted to investigating and building-up new material models like anisotropic creep laws or continuum damage mechanics. The researches usually show that the models with various assumptions affect in a serious way differences of material behaviour and should be used in designing structures. Nevertheless, the models are sophisticated and not "easy-going"

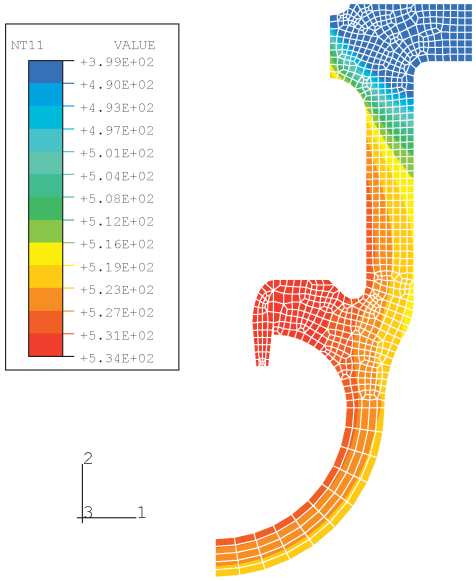

Figure 8. Steady state temperature field calculated by ABAQUS in [K]

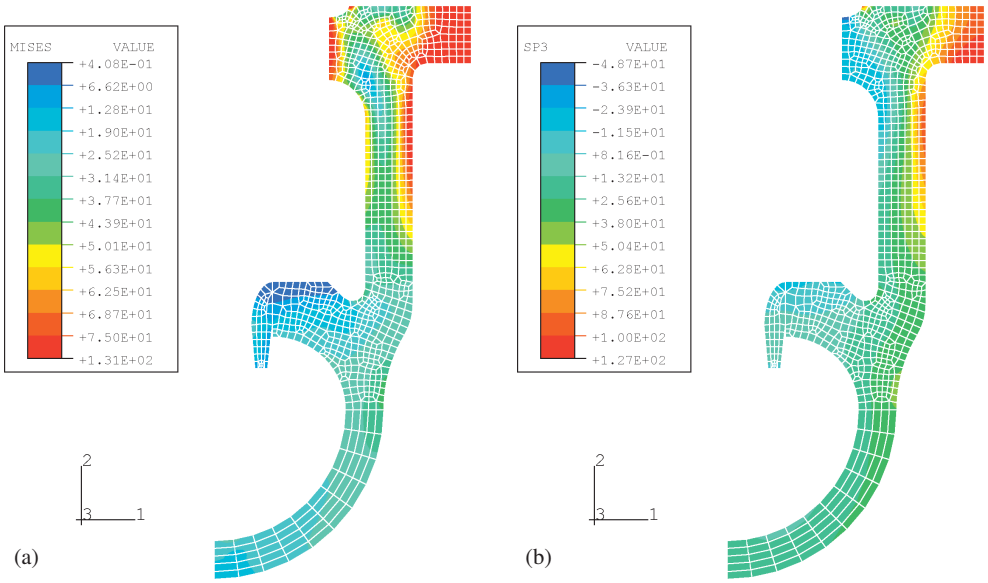

Figure 9. (a) Von Mises stress σ_{HMH} and (b) maximal principal stress σ_3 [MPa] for thermal steady state without creep

for ordinary engineers unless the calculations are carried out with computer programs. The stress state of common hardware is quite complex and may change during long-term service on virtue of shake down or relaxation which may compensate the differences coming from set-up of the diverse constitutive laws.

With creep data obtained from creep testing [10, 6], the analysis of creep after the cold start-up and normal operating conditions has been performed. Owing to inelastic creep

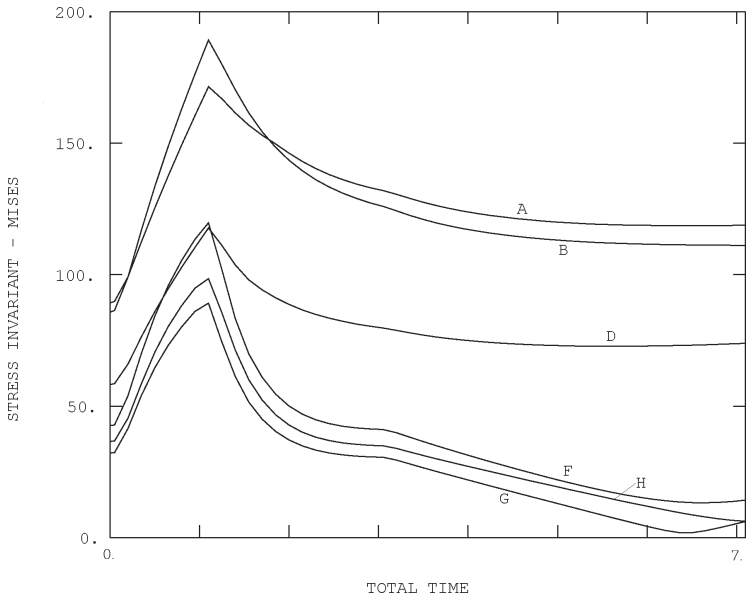

Figure 10. Change of the equivalent HMH stress [MPa] during start-up in the ctitical elements

deformations (Figure 11b), a strong redistribution in the stress state has been observed (Figure 11a). After every cycle: start-up – creep via 10^6 hours – shutdown, a significant redistribution of the residual stresses was easily observed. Respectively to creep evolution, according to formulae (17), growth of the creep damage parameter ω was observed. However, the total damage, due to low-cyclic fatigue, should be a sum of the fatigue damage and the creep damage.

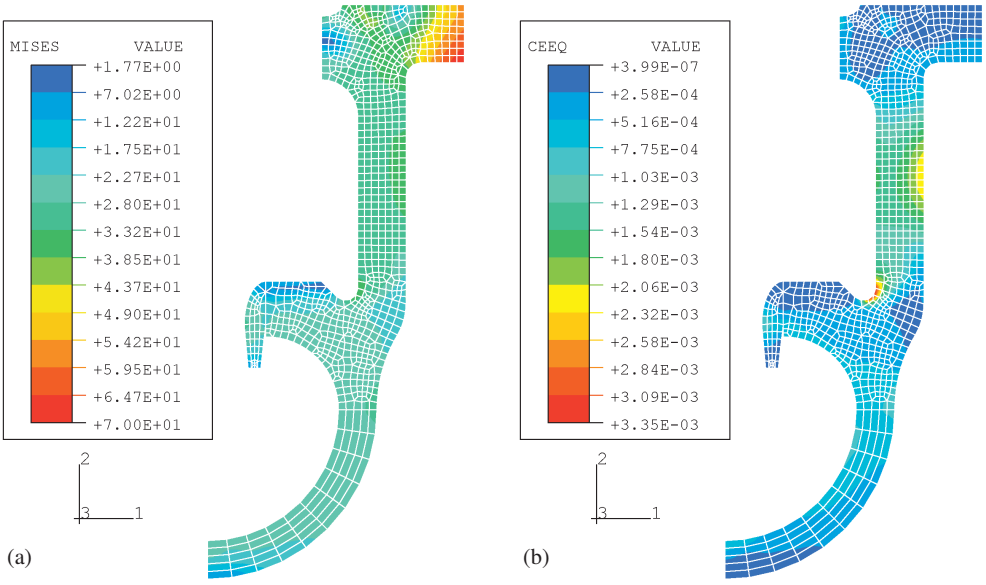

Figure 11. (a) Von Mises stress σ_{HMH} [MPa] for hot state with creep after 10^6 h; (b) equivalent creep strain after 10^6 h

6. Life-time prediction

The main steam pipeline valve tends to work in open state, this means, that the temperature of the stream flow is almost steady during service. Hence the structure is loaded by [7]:

- pressure 180 bar of the flowing steam; there is some additional dynamic part in the diffuser region,
- temperature of steam (535°C) inside and common temperature outside (20°C); some part of outside surface is isolated,
- the lid of valve is bolded to the trunk of valve – this gives self-balanced constant loading in the top part of the structure.

The gravity load and forces from moving parts are neglected during analysis. The thick walls and large mass of structure is the reason for thermo-mechanical low-cyclic fatigue. The fast heating up during several hours to 530°C causes great strain ($\sim 0.7\,\%$). However this is more than yield strain ($\sim 0.2\,\%$), the strain amplitude is in reversible region of elastic stresses and thermal expansion. From the point of view of lifetime prediction, it has been arbitrarily assumed that the maximal principal strain amplitude is a 3D equivalent of the uniaxial strain amplitude during fatigue test.

Quite low stresses during steady state service in comparison to the stresses during start up is the other reason that the creep of metal is small and does not affect the life-time in any visible way (see Figure 9). Despite the small creep, one can see the stress relaxation. This behaviour takes place during the whole service time of valve (see Figure 9 and Figure 10). The simulation of turbine start-up and shutdown shows some reduction of maximal stress amplitude (primary and tensor components) – see Figure 12.

The conclusion is that the stress relaxation (creep), or likely shakedown (plasticity), do not improve the lifetime of the fatigue structure. The places most endangered by fatigue are points B and F from Figure 12. Those two places are most frequently reported by in-situ investigations as well as indicated by numerical simulation as this one and others [15]. It should be added that the localisation of stress maximum in the top part of valve is strongly affected by the thermal boundary condition, what is not easy to model on numerous surfaces. As already said, the strain amplitude during loading – unloading is about 0.7 %. For such strain cycling range the steel L21HMF (see arrow on Figure 14) has fatigue cycle limit 500–3000 cycles. This is within the spread of lifetime of valves in service.

7. Conclusions

A complex, advanced CFD-CSM, calculation of the whole cut-off valve of the 200 MW Unit of Steam Power Plant has successfully been performed. The methodology for low-cyclic fatigue life prediction, integrating advanced CFD and CSM technology, provides a valuable tool for the design and improved maintenance management of power plants elements. Furthermore, in the case of old and degraded elements a systematic approach to refurbishment is possible even if there is more then 1000 start-ups and shut downs. The methodology described here is well suited to predict the service life of critical elements of a power plant unit and to aid engineer designers in avoiding structural failure. The expected major effects are due to fatigue caused by start-up and shutdown operation with the high rate of temperature gradients.

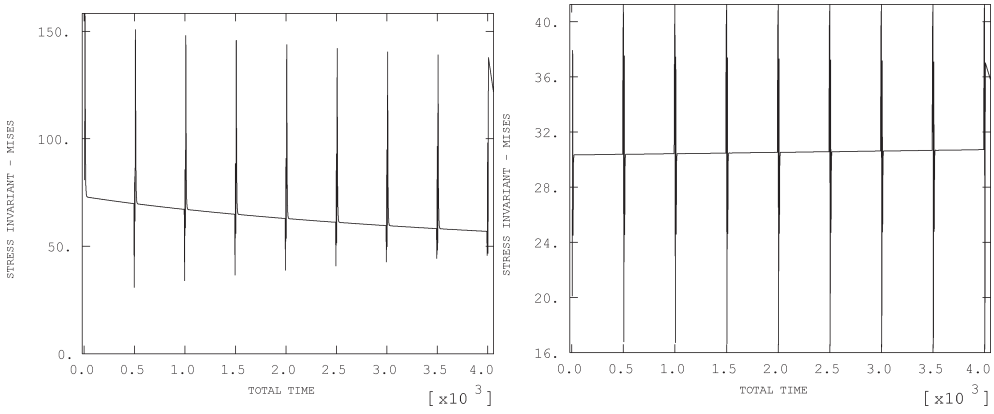

B F

Figure 12. Equivalent von Mises stress σ_{HMH} [MPa] during service time [h]

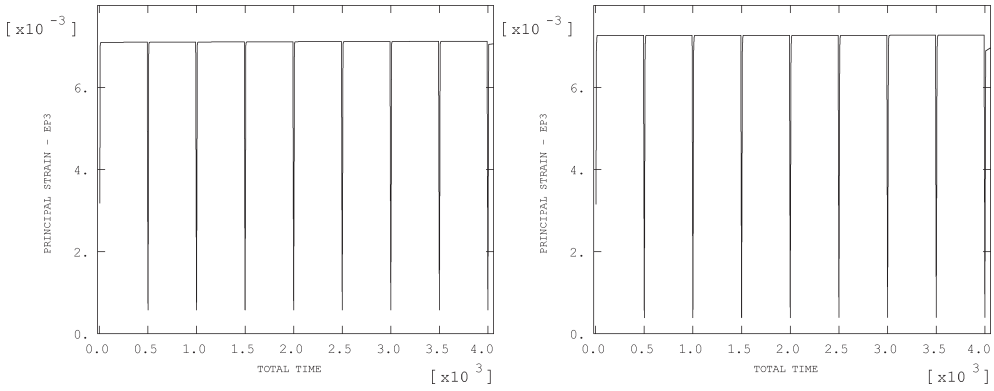

B F

Figure 13. Maximal principal strain ε_3 [%] during service time [h]; stress and strain during cycling loading from cold state including creep; *B* and *F* points from Figure 12

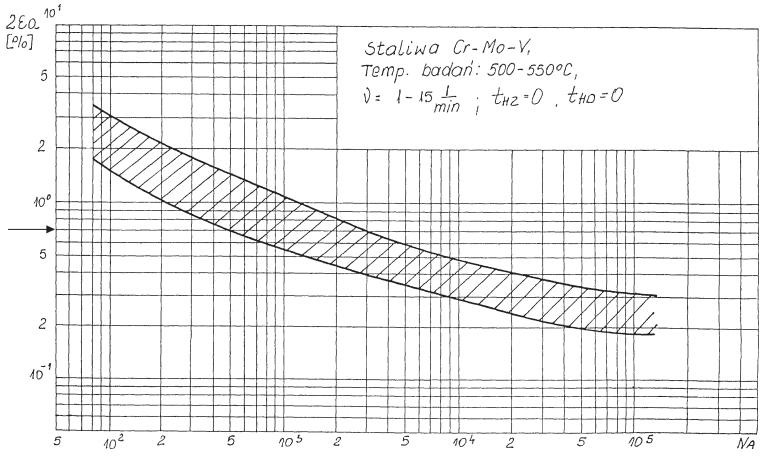

Figure 14. Fatigue limit of CrMoV cast steel in temperature 500–550°C [3]

Acknowledgements

This investigation was supported by TASK – Academic Computer Centre in Gdansk.

References

[1] Dejean F 1995 *Aerodynamic – thermomechanic coupling and creep – fatigue damage prediction. Part A: Aerodynamic investigation* In PWR **28** JPGC ASME Minneapolis, pp. 301–307
[2] Bruchet Ph 1995 *Aerodynamic – thermomechanic coupling and creep – fatigue damage prediction. Part B: Thermomechanic investigation* In PWR **28** JPGC ASME Minneapolis, pp. 308–320
[3] Chmielniak T, Kosman G and Rusin A 1990 *Creep of elements of steam turbines* WNT (in Polish)
[4] Radulski W, Bielecki M, Karcz M and Badur J 2000 *National Conference – Energetyka'2000*, Wrocław, pp. 39–48 (in Polish)
[5] Badur J, Banaszkiewicz M, Karcz M and Winowiecki M 1999 *Proceed. of Int. Conf. SYMKOM'99*, Lódź, *Turbomachinery* **115** 31
[6] Radulski W, Bielecki M, Karcz M and Badur J 2000 *Int. Con. Scient. and Tech. Vitebsk* p. 243 (in Russian)
[7] Badur J, Bielecki M, Karcz M and Radulski W 1999 *Raport IMP PAN* no. 358/99 p. 1–29 (in Polish)
[8] ABAQUS Theory Manual ver. 5.5 USA 1995 Hibbitt, Karlsson and Sorensen Inc.
[9] FLUENT User's Guide, Fluent Inc., 1997–1999
[10] Bielecki M and Badur J 1999 *28th National Conference on Nondestructive Measurements* p. 143 (in Polish)
[11] Bielecki M 1999 www.imp.pg.gda.pl/fem
[12] Bielecki M, Badur J and Wiśniewski G 2000 *Zeszyty Naukowe IMP PAN* 507/1466/2000 (in Polish)
[13] Karcz M 1999 *Raport IMP PAN* no. 519/99 pp. 1–20 (in Polish)
[14] Launder B E and Spalding D B 1974 *Computer Methods in Applied Mechanics and Engineering* **3** 269
[15] Rusin A and Daciuk Ł 1998 *Zeszyty Naukowe Politechniki Śląskiej, Seria: Energetyka* 130 (in Polish)